Bol. Soc. Paran. Mat.
©SPM – E-ISSN-2175-1188
SPM: www.spm.uem.br/bspm

(3s.) **v. 2026 (44) 6** : 1–20.
ISSN-0037-8712
doi:10.5269/bspm.79045

# Nonlinear Dynamics of Allee Effect and Fear in a Delayed Diffusive Predator-Prey Model

Mohamed HAFDANE, Asmaa IDMBAREK, Nossaiba BABA and Youssef EL FOUTAYENI

ABSTRACT: This paper investigates the dynamics of a predator–prey model incorporating both the Allee effect and predator-induced fear, along with a delay representing the time required for prey to develop anti-predation defenses. The model also includes diffusion terms to account for species movement and considers harvesting pressure on both populations. We first establish the existence and local stability of the coexistence equilibrium, then analyze the conditions under which a delay-induced Hopf bifurcation occurs. Using center manifold theory and normal form analysis, we characterize the direction, stability, and periodicity of the bifurcating solutions. Numerical simulations are conducted to validate the theoretical predictions and reveal rich dynamics, including transitions from stability to periodic oscillations and the emergence of spatial patterns due to asymmetric diffusion. These results highlight the critical role of delayed behavioral responses and spatial heterogeneity in shaping ecological stability.

Keywords: Predator-Prey, stability analysis, Hopf bifurcation, diffusion, normal form, harvesting.

## Contents



## 1. Introduction

The dynamic relationship between predators and their prey is a central topic in ecology, playing a fundamental role in population dynamics. Over the past three decades, extensive research has been conducted on predator–prey models, leading to the development of more realistic frameworks based on laboratory experiments and field observations. Understanding these interactions is essential for comprehending ecosystem dynamics. In this relationship, the predator depends on the prey as a food source, while the prey must defend itself against predation to ensure its survival and reproduction. These interactions have major repercussions not only on predator and prey populations but also on the overall structure and functioning of ecosystems [1], [12], [24], [25], [26], [27], [32], [33].

The analysis of stability and bifurcations is essential for understanding the dynamics of predator–prey systems and their sensitivity to parameter variations. In particular, the Hopf bifurcation plays a key role in the emergence of periodic oscillations, reflecting the natural fluctuations of populations. Recent studies have explored various factors influencing this bifurcation. Patra et al. (2021) demonstrated the impact of defensive behaviors and gestation delays [13], while Ghimire and Wang (2021) showed that the Hopf bifurcation in a cooperative predation context is always supercritical [14]. Yao et al. (2021) analyzed the

2020 *Mathematics Subject Classification:* 91B05, 91A06, 91B02, 91B50.
Submitted September 18, 2025. Published February 17, 2026

effects of cooperative hunting and a Holling type III functional response on dynamic transitions [15], and Lv (2022) highlighted the influence of memory and gestation delays in a diffusive model [16]. These studies emphasize the importance of Hopf bifurcation analysis in characterizing ecosystem dynamic regimes and in better understanding their stability in the face of environmental disturbances.

The Allee effect is a biological phenomenon that strongly influences population dynamics. Described by Warder Clyde Allee (1931), it represents a positive correlation between population density and growth rate when numbers are low. Mathematically, this effect can be modeled by the following equation:

$$\dot{H}(t) = H\left(\frac{aH}{b+H} - c - dH\right), \tag{1.1}$$

where $H(t)$ represents the prey density, $a$ is the maximum growth rate, $b$ represents the intensity of the Allee effect, $c$ is the mortality rate, and $d$ denotes the effect of density on growth. This phenomenon has been extensively studied in various contexts, notably in single-species models and host–parasitoid interactions [28]. In 2007, Janga and Diamond [29] showed that in discrete-time models, a high intrinsic growth rate could generate chaotic dynamics or even lead to extinction when the population falls below a critical threshold. In a predator–prey framework, several studies have examined the Allee effect. For example, in 2009, the authors [30] demonstrated that integrating this effect stabilized prey populations. In 2016, another study [2] deepened this analysis by incorporating the impact of human predation on predators and prey, highlighting the existence and stability of the positive equilibrium. Recent contributions have further explored the Allee effect in combination with harvesting and spatial dynamics [34], [36].

Another factor influencing population dynamics is predator-induced fear. Experimental studies have shown that the presence of predators alters prey behavior, prompting them to reduce their feeding activity and avoid risky areas, which can negatively affect their growth rate. For instance, Zanette et al. (2011) [3] observed a 40% reduction in reproductive success in song sparrows exposed to predator cues. From a theoretical perspective, Wang et al. (2016) [4] developed a predator–prey model incorporating fear, showing that this effect could stabilize population dynamics by reducing oscillations. Pandey et al. (2020) [5] later extended these results by introducing fear dynamics into a three-trophic-level model based on the Hastings–Powell framework, demonstrating that adjusting the fear parameter could control chaotic system behavior

These two effects can be combined in a single mathematical framework to model their interaction on population dynamics. Thus, the Allee effect is modified to include predator-induced fear, leading to the following expression:

$$\dot{H}(t) = H\left(\frac{aH}{(b+H)(1+fS)} - c - dH\right), \tag{1.2}$$

where the term $(1 + fS)$ represents the effect of predator-induced fear on prey growth, with $f$ reflecting the intensity of this fear as a function of predator density $S$.

Predator–prey interactions are also strongly influenced by the defensive strategies adopted by prey to reduce predation risk. Several studies have explored the impact of these mechanisms on population dynamics. For example, Tang and Xiao (2015) [10] analyzed a model incorporating active anti-predation behavior, where adult prey counterattack vulnerable predators, revealing complex bifurcations such as Hopf and Bogdanov–Takens bifurcations. Similarly, Sun et al. (2016) [11] studied a system in which anti-predation behavior depended on a prey density threshold, uncovering bistability and tristability dynamics. However, these studies generally assume an immediate prey response, which does not always reflect ecological reality.

In our model, we introduce a new approach by considering a delayed anti-predation mechanism. Indeed, in many ecosystems, prey do not react instantly to predator presence but develop defense mechanisms after a certain delay. This phenomenon may correspond, for example, to the time required for

toxin production, the adoption of defensive behaviors, or the learning of avoidance strategies. Unlike previous works, we introduce a delay $\tau$ to represent this biological latency, reflecting the fact that the anti-predation effect manifests only after a certain time. This dynamic is modeled by the term $g_3H(t-\tau)S$.

Another factor influencing system dynamics is the fishing pressure exerted on both species. Overexploitation of resources can disrupt population balance and alter ecological interactions. We model this effect using the terms $E_1H$ and $E_2S$, representing the fishing effort applied to prey and predators, respectively. Including these terms allows us to assess the impact of human activities on the viability of the studied populations. Recent studies have highlighted the importance of incorporating harvesting effort in predator–prey systems with Allee effect and fear [33].

Classical models based on ordinary differential equations often neglect the effects of spatial dispersion among individuals. To better capture ecological heterogeneity, we introduce partial differential equations (PDEs), which allow us to model population movement in space. The inclusion of diffusion terms makes it possible to study the effects of spatial heterogeneity on predator–prey dynamics, considering individual displacements in response to local density and resource variations. This approach provides a more comprehensive understanding of ecological interactions by integrating both temporal and spatial dynamics.

The studied model is thus defined by the following system:

$$\begin{cases} \frac{\partial H(x,t)}{\partial t} = d_1\Delta H + H\left(\frac{aH}{(b+H)(1+fS)} - c - dH\right) - g_1HS - E_1H, \\ \frac{\partial S(x,t)}{\partial t} = d_2\Delta S + g_2SH - mS - g_3H(t-\tau)S - E_2S, \\ \frac{\partial H(x,t)}{\partial \nu} = \frac{\partial S(x,t)}{\partial \nu} = 0, \quad \forall x \in \partial\Omega, \forall t > 0 \\ H(x,t) = H_1(x,t) \geq 0, \quad S(x,t) = S_1(x,t) \geq 0, \quad x \in \Omega, t \in [-\tau, 0]. \end{cases} \tag{1.3}$$

The parameters of the model are defined in the following table:

Table 1: Meaning of model parameters

| Parameter | Meaning |
|---|---|
| $a$ | Maximum filtering capacity per individual in the population. |
| $b$ | Intensity of the Allee effect |
| $c$ | Prey mortality rate |
| $d$ | Intensity of intraspecific competition |
| $f$ | Intensity of predator-induced fear |
| $g_1$ | Prey mortality rate due to predation. |
| $g_2$ | Predator reproduction rate based on encountered prey. |
| $m$ | Predator mortality rate |
| $g_3$ | Intensity of the prey's anti-predation behavior against predators. |
| $\tau$ | Time required for the development of anti-predation defenses. |
| $d_1$, $d_2$ | Diffusion coefficients |
| $E_1$, $E_2$ | Fishing effort level applied to target species. |

This work makes an original contribution to the study of predator-prey systems by analyzing the stability of the model as a function of the delay $\tau$, which represents the time required for the development of prey defense mechanisms. In particular, we explore how this delay can influence the emergence of oscillations in population dynamics through a Hopf bifurcation analysis. This approach allows identifying critical thresholds where the system behavior changes radically, highlighting the importance of delayed effects in ecological interactions.

The structure of the paper is organized as follows. Section 2 establishes the existence and boundedness of solutions. Section 3 investigates the stability of the coexistence equilibrium and identifies the conditions under which a Hopf bifurcation arises, marking the onset of oscillatory dynamics. Section 4 provides a

detailed analysis of the bifurcation properties, focusing on the qualitative features of the emerging periodic solutions. Section 5 presents numerical simulations that illustrate how the delay parameter shapes the system's dynamical behavior. Section 6 concludes the paper by summarizing the main findings.

## 2. Existence and Boundedness of the Solution

**Theorem 2.1** *Assume that the initial data satisfy $H_1(x,t) \geq 0$ and $S_1(x,t) \geq 0$. Then system (1.3) admits a unique positive solution $(H(x,t), S(x,t))$ defined for all $x \in \Omega$ and $t > 0$. Moreover, the solution is uniformly bounded in $\Omega \times (0,\infty)$ and fulfills*

$$\limsup_{t\to+\infty} H(x,t) \leq \frac{a}{d}, \qquad \|H(\cdot,t)\|_{C(\overline{\Omega})} \leq C_1, \qquad \|S(\cdot,t)\|_{C(\overline{\Omega})} \leq C_2,$$

*where $C_1 = \max\left\{\frac{a}{d}, \max_{\overline{\Omega}} H_1(x)\right\}$ and $C_2$ depends on $C_1$, $|\Omega|$, and the initial data.*

**Proof:** We first define

$$\varphi(H,S) = H\left(\frac{aH}{(b+H)(1+fS)} - c - dH\right) - g_1HS - E_1H,$$
$$\psi(H,S) = g_2SH - mS - g_3H(t-\tau)S - E_2S.$$

The partial derivatives

$$\varphi_S = -\frac{afH^2}{(b+H)(1+fS)^2} - g_1H \leq 0, \qquad \psi_H = g_2S \geq 0$$

show that the system is mixed quasimonotone in $\overline{\mathbb{R}^2_+} = \{(H,S) : H \geq 0, S \geq 0\}$. This property ensures the existence of ordered upper and lower solutions. Let us consider the corresponding delayed ODE system

$$\begin{cases} \dot{H}(t) = H\left(\dfrac{aH}{(b+H)(1+fS)} - c - dH\right) - E_1H, \\ \dot{S}(t) = g_2SH - mS - g_3H(t-\tau)S - E_2S, \\ H(t) = \overline{H_1}, \quad S(t) = \overline{S_1}, \quad t \in [-\tau, 0], \end{cases} \tag{2.1}$$

where $\overline{H_1} = \sup_{\overline{\Omega}} H_1(x,t)$ and $\overline{S_1} = \sup_{\overline{\Omega}} S_1(x,t)$. Let $(\tilde{H}, \tilde{S})$ denote the unique positive solution of (2.1). By standard comparison arguments, the solution $(H,S)$ of system (2.1) satisfies

$$0 \leq H(x,t) \leq \tilde{H}(t), \qquad 0 \leq S(x,t) \leq \tilde{S}(t), \quad \forall (x,t) \in \Omega \times (0,\infty). \tag{2.2}$$

The strong maximum principle further implies that $H(x,t) > 0$ and $S(x,t) > 0$ for all $t > 0$.

To obtain the upper bound of $H$, note that

$$\frac{\partial H}{\partial t} - d_1\Delta H = H\left(\frac{aH}{(b+H)(1+fS)} - c - dH\right) - g_1HS - E_1H \leq H(a - dH).$$

By the parabolic comparison principle, we deduce

$$\limsup_{t\to+\infty} \max_{\overline{\Omega}} H(x,t) \leq \frac{a}{d}.$$

Hence, $\|H(\cdot,t)\|_{C(\overline{\Omega})} \leq C_1$ for all $t \geq 0$.

We now establish the boundedness of $S$. Let

$$h(t) = \int_\Omega H(x,t)\,dx, \qquad s(t) = \int_\Omega S(x,t)\,dx.$$

Integrating the system over $\Omega$ and using the Neumann boundary conditions, we obtain

$$\frac{dh(t)}{dt} = \int_\Omega H\left(\frac{aH}{(b+H)(1+fS)} - c - dH - g_1 S - E_1\right)dx,$$
$$\frac{ds(t)}{dt} = \int_\Omega S\left(g_2 H - m - g_3 H(t-\tau) - E_2\right)dx.$$

By summing the two relations, we get

$$\frac{d}{dt}\left(\frac{g_2}{g_1}h + s\right) \leq -m\left(\frac{g_2}{g_1}h + s\right) + \frac{g_2}{g_1}(a+m)\,C_1|\Omega|. \tag{2.3}$$

Applying Gronwall's inequality to (2.3) yields

$$\int_\Omega S(x,t)\,dx \leq \left(\frac{g_2}{g_1}h(0) + s(0)\right)e^{-mt} + \frac{\frac{g_2}{g_1}(a+m)\,C_1|\Omega|}{m}(1-e^{-mt}).$$

Therefore,

$$\|S(\cdot,t)\|_{L^1(\Omega)} \leq \frac{g_2}{g_1}\|H_1\|_{L^1(\Omega)} + \|S_1\|_{L^1(\Omega)} + \frac{\frac{g_2}{g_1}(a+m)\,C_1|\Omega|}{m}.$$

By the uniform $L^1$–boundedness and the local Lipschitz continuity of $\psi(H,S)$, the application of the regularity result of Aliakakos [31] ensures that

$$\|S(\cdot,t)\|_{L^\infty(\Omega)} \leq C_2.$$

Combining these estimates completes the proof. □

## 3. Stability Analysis

### 3.1. Equilibrium points

The main aim of this section is to identify the conditions under which a strictly positive equilibrium point, characterized by the coexistence of both species, can exist.

**Theorem 3.1** *assuming that*

$$(c + E_1 + dH^*)(b + H^*) - aH^* < 0 \tag{3.1}$$

*If the condition stated holds, then the system (1.3) possesses a single and exclusive equilibrium point $(H^*, S^*)$ that is strictly positive.*

**Proof:** To search this equilibrium, we solve the following equations

$$\begin{cases} \frac{aH}{(b+H)(1+fS)} - c - dH - g_1 S - E_1 = 0 \\ -m + g_2 H - g_3 H - E_2 = 0 \end{cases}$$

Solving the second equation is equivalent to

$$H^* = \frac{E_2 + m}{g_2 - g_3} \tag{3.2}$$

And according to the first equation, $S^*$ is the solution of

$$A_2 S^{*2} + A_1 S^* + A_0 = 0 \tag{3.3}$$

where

$$A_2 = (b + H^*)g_1 f$$
$$A_1 = (b + H^*)(fc + fE_1 + fdH^* + g_1)$$
$$A_0 = (c + E_1 + dH^*)(b + H^*) - aH^*$$

It is evident that both $A_2$ and $A_1$ are positive. Therefore, Equation (3.3) possesses a unique positive solution $S^*$ if and only if $A_0 < 0$, i.e.,$(c + E_1 + dH^*)(b + H^*) - aH^* < 0$. □

### 3.2. Stability

The main objective of this section is to analyze the stability and bifurcations of system (1.3) based on the delay parameter [17], [18], [20]. The first step in this analysis involves linearizing the system at the equilibrium point $(H^*, S^*)$, we get

$$\frac{\partial H(t)}{\partial t} = d\Delta H(t) + MH(t) + NH(t-\tau)$$

where

$$H(t) = \begin{pmatrix} H(t) \\ S(t) \end{pmatrix}, \quad d = \begin{pmatrix} d_1 & 0 \\ 0 & d_2 \end{pmatrix}, \quad M = \begin{pmatrix} m_{11} & m_{12} \\ g_2 S^* & 0 \end{pmatrix}, \quad N = \begin{pmatrix} 0 & 0 \\ -g_3 S^* & 0 \end{pmatrix},$$

and

$$m_{11} = \frac{abH^*}{(H^* + b)(1 + fS^*)} - dH^*, \quad m_{12} = \frac{-af(H^*)^2}{(H^* + b)(1 + fS^*)^2} - g_1 H^*.$$

**Characteristic equation**

We consider the following equation

$$\det\left(\lambda I - D_n - M - Ne^{-\lambda\tau}\right) = 0$$

where

$$I = \begin{pmatrix} 1 & 0 \\ 0 & 1 \end{pmatrix}, \quad \textit{and} \quad D_n = -n^2/l^2 \begin{pmatrix} d_1 & 0 \\ 0 & d_2 \end{pmatrix}.$$

By solving the previous equation, we get the characteristic equation corresponding to system (1.3)

$$\lambda^2 + S_n\lambda + F_n + Ce^{-\lambda\tau} = 0, \tag{3.4}$$

where

$$\begin{aligned} S_n &= (d_1 + d_2)\frac{n^2}{l^2} - m_{11} \\ F_n &= \frac{n^4}{l^4} d_1 d_2 - m_{11} d_2 \frac{n^2}{l^2} - m_{12} g_2 v^* \\ C &= m_{12} g_3 v^* \end{aligned}$$

**Without delay**

For $\tau = 0$, the characteristic equation becomes as follows

$$\lambda^2 + S_n\lambda + F_n + C = 0$$

If $F_n + C > 0$ and $S_n > 0$, then the system without delays is locally asymptotically stable around the equilibrium point $(H^*, S^*)$.

**With delay**

Assuming that the characteristic equation admits a pair of purely imaginary roots$\pm i\omega(\omega > 0)$, we can separate the real and imaginary parts of this equation, which leads to the following system

$$\begin{cases} \omega^2 - F_n = C\cos\omega\tau, \\ -S_n\omega = -C\sin\omega\tau. \end{cases}$$

Thus,

$$\cos\omega\tau = \frac{\omega^2 - F_n}{C} \quad \text{and} \quad \sin\omega\tau = \frac{S_n\omega}{C}$$

Which implies that

$$\omega^4 + \left(S_n^2 - 2F_n^2\right)\omega^2 + F_n^2 - C^2 = 0.$$

Let $\eta = \omega^2$, then the above equation can be rewritten in the form:

$$F(\eta) = \eta^2 + \left(S_n^2 - 2F_n^2\right)\eta + F_n^2 - C^2.$$

The equation $F(\eta) = 0$ :

- Has no positive roots if $S_n^2 - 2F_n^2 < 0$.
- Has one unique positive root, if $F_n^2 - C^2 < 0$ holds.
- Has two positive roots, if $S_n^2 - 2F_n^2 < 0, \quad F_n^2 - C^2 > 0, \ \left(S_n^2 - 2F_n^2\right)^2 - 4\left(F_n^2 - C^2\right)^2 > 0$ holds.

For the last case, the critical delay is expressed as follows:
for $l = 0, 1, 2, \ldots$ and $k = 0, 1, 2, \ldots$

$$\tau_l^{(k)} = \begin{cases} \frac{1}{\omega_l}\left[\arccos\left(\frac{\omega_l^2 - F_n}{C}\right) + 2k\pi\right], & \text{if } \omega_l^2 - F_n > 0, \\ \frac{1}{\omega_l}\left[2\pi - \arccos\left(\frac{\omega_l^2 - F_n}{C}\right) + 2k\pi\right], & \text{if } \omega_l^2 - F_n < 0 \end{cases}$$

Now, applying the transversality conditions leads to:

$$\begin{aligned} \Re\left[\frac{d\lambda}{d\tau}\right]^{-1}_{\tau=\tau_l^{(k)}} &= \Re\left(\frac{2\lambda + S_n}{C\lambda e^{-\lambda\tau}} - \frac{\tau}{\lambda}\right) \\ &= \frac{S_n^2 w^2 + 2w^2\left(w^2 - F_n\right)}{S_n^2 w^4 + \left(w^3 - F_n w\right)^2} \\ &= \frac{\sqrt{\left(S_n^2 - 2F_n\right)^2 - 4\left(F_n^2 - C^2\right)}}{w^4 + F_n^2 + \left(S_n^2 - 2F_n\right)w^2} > 0. \end{aligned}$$

Consequently, we can deduce that for $\tau > \tau_l^{(k)}$, there exists at least one eigenvalue with a non-negative real part. Furthermore, the conditions required for a Hopf bifurcation to occur are also essential in demonstrating the presence of periodic solutions.

**Theorem 3.2** *For system (1.3)*

- *If the condition $S_n^2 - 2F_n^2 < 0$ holds, the equilibrium is locally asymptotically stable for all $\tau > 0$.*
- *If the condition $F_n^2 - C^2 < 0$ is satisfied, the equilibrium is locally asymptotically stable for $0 < \tau < \tau_0^0$ and unstable for $\tau > \tau_0^0$. Moreover, the system undergoes a Hopf bifurcation at $\tau = \tau_0^{(k)}$ for $k = 0, 1, 2, \ldots$.*

- *If the conditions* $S_n^2-2F_n^2<0$, $F_n^2-C^2>0$, *and* $\left(S_n^2-2F_n^2\right)^2-4\left(F_n^2-C^2\right)^2>0$ *are satisfied, then there exists* $m\in\mathbb{N}$ *such that: The equilibrium is locally asymptotically stable for* $\tau\in\left[0,\tau_2^{(0)}\right)\cup\bigcup_{j=0}^{m-1}\left(\tau_1^{(j)},\tau_2^{(j+1)}\right)$. *The equilibrium is unstable for* $\tau\in\bigcup_{j=0}^{m-1}\left(\tau_2^{(j)},\tau_1^{(j)}\right)\cup\left(\tau_2^{(m)},+\infty\right)$. *The system (1.3) undergoes a Hopf bifurcation at* $E_2$ *when* $\tau=\tau_l^{(k)}$, *where* $l=1,2$, *and* $k=0,1,2,\cdots$.

## 4. Hopf Bifurcation

Our objective in this section is to achieve the normal form of Hopf bifurcation for the interior equilibrium. To do this, we introduce new variables $\bar{H}(x,t)$ and $\bar{S}(x,t)$, defined as deviations from their steady-state values: $\bar{H}(x,t)=H(x,\tau t)-H^*$ and $\bar{S}(x,t)=S(x,\tau t)-S^*$. For the sake of convenience, we will omit the bars in the subsequent equations. Consequently, the resulting system becomes:

$$\begin{cases}\frac{\partial H(x,t)}{\partial t}=\tau\left[d_1\Delta H+(H+H^*)\left(\frac{a(H+H^*)}{(b+(H+H^*))(1+f(S+S^*))}-c-d(H+H^*)-g_1(S+S^*)-E_1\right)\right],\\ \frac{\partial S(x,t)}{\partial t}=\tau\left[d_2\Delta S+(S+S^*)\left(-m+g_2(H+H^*)-g_3(H(t-1)+H^*)-E_2\right)\right]\end{cases}$$

Let us introduce the notations: $\tau=\tilde{\tau}+\varepsilon$, and $H=(H(x,t),S(x,t))^T$. The phase space $C:=C([-1,0],X)$ can then be reformulated as follows:

$$\frac{\mathrm{d}H(t)}{\mathrm{d}t}=\tilde{\tau}D\Delta H(t)+L_{\tilde{\tau}}(H_t)+P(H_t,\varepsilon),$$

where

$$L_\varepsilon(\chi)=\varepsilon\begin{pmatrix}m_{11}\chi_1(0)+m_{12}\chi_2(0)\\ g_2S^*\chi_1(0)+-g_3S^*\chi_1(-1)\end{pmatrix}$$

and

$$P(\chi,\varepsilon)=\varepsilon D\Delta\chi+L_\varepsilon(\chi)+p(\chi,\varepsilon),$$

such that

$$p(\chi,\varepsilon)=(\tilde{\tau}+\varepsilon)\left(p_1(\chi,\varepsilon),p_2(\chi,\varepsilon)\right)^T,$$

with

$$\begin{aligned}p_1(\chi,\varepsilon) &= \frac{a(\chi_1(0)+H^*)^2}{(b+(\chi_1(0)+H^*))(1+f(\chi_2(0)+S^*))}-c(\chi_1(0)+H^*)-d(\chi_1(0)+H^*)^2\\ &\quad -g_1(\chi_1(0)+H^*)(\chi_2(0)+S^*)-E_1(\chi_1(0)+H^*)+m_{11}\chi_1(0)+m_{12}\chi_2(0)\\ p_2(\chi,\varepsilon) &= -m(\chi_2(0)+S^*)+g_2(\chi_1(0)+H^*)(\chi_2(0)+S^*)-g_3(\chi_1(-1)+H^*)(\chi_2(0)+S^*)\\ &\quad -E_2(\chi_2(0)+S^*)+g_2S^*\chi_1(0)-g_3S^*\chi_1(-1)\end{aligned}$$

Respectively, for $\chi=(\chi_1,\chi_2)^T\in C_1$. We know that $\Lambda_n:=\{i\omega_n\tilde{\tau},-i\omega_n\tilde{\tau}\}$ are characteristic roots of

$$\frac{\mathrm{d}x(t)}{\mathrm{d}t}=-\tilde{\tau}D\frac{n^2}{l^2}x(t)+L_{\tilde{\tau}}(x_t)$$

The application of the Riesz representation theorem allows us to establish the existence of a $2\times2$ matrix function $\eta^n(s,\tilde{\tau}),(-1\le s\le0)$, whose elements are functions with bounded variation such that

$$-\tilde{\tau}D\frac{n^2}{l^2}\chi(0)+L_{\tilde{\tau}}(\chi)=\int_{-1}^{0}d\eta^n(s,\tau)\chi(s)\quad\text{for}\chi\in C\left([-1,0],\mathbb{R}^2\right).$$

Choose

$$\eta^n(s,\tau)=\begin{cases}-\tau F & s=-1\\ 0 & s\in(-1,0)\\ \tau E & s=0\end{cases}$$

where

$$E = \begin{pmatrix} m_{11} - d_1 \frac{n^2}{l^2} & m_{12} \\ g_2 S^* & -d_2 \frac{n^2}{l^2} \end{pmatrix}, \qquad F = \begin{pmatrix} 0 & 0 \\ -g_3 S^* & 0 \end{pmatrix}$$

We define

$$(\psi, \chi) = \psi(0)\chi(0) - \int_{-1}^{0} \int_{\xi=0}^{s} \psi(\xi - s) d\eta^n(s, \tilde{\tau}) \chi(\xi) d\xi \quad \text{for} \chi \in C\left([-1, 0], \mathbb{R}^2\right), \psi \in C\left([0, 1], \mathbb{R}^2\right).$$

$A(\tilde{\tau})$ has two distinct purely imaginary eigenvalues. $\pm i\omega_n \tilde{\tau}$, they are eigenvalues of $A^*$.
Define $l_1(s) = (1, \zeta)^T e^{i\omega_n \tilde{\tau} s} \quad (s \in [-1, 0]), \quad n_1(r) = (1, \vartheta) e^{-i\omega_n \tilde{\tau} r} \quad (r \in [0, 1])$, where

$$\zeta = \frac{1}{m_{12}} \left( -m_{11} + d_1 \frac{n^2}{l^2} + i\omega_n \right),$$

$$\vartheta = \frac{e^{-i\tilde{\tau}\omega_n}}{(g_2 - g_3) S^*} \left( -m_{11} + d_1 \frac{n^2}{l^2} - i\omega_n \right)$$

Let $\Theta = (\Theta_1, \Theta_2)$ and $\kappa^* = (\kappa_1^*, \kappa_2^*)^T$ with

$$\begin{aligned} \Theta_1(s) &= \tfrac{l_1(s) + l_2(s)}{2} = \begin{pmatrix} \operatorname{Re}\left(e^{i\omega_n \tilde{\tau} s}\right) \\ \operatorname{Re}\left(\zeta e^{i\omega_n \tau s}\right) \end{pmatrix} \\ \Theta_2(s) &= \tfrac{l_1(s) - l_2(s)}{2i} = \begin{pmatrix} \operatorname{Im}\left(e^{i\omega_n \tilde{\tau} s}\right) \\ \operatorname{Im}\left(\zeta e^{i\omega_n \tilde{\tau} s}\right) \end{pmatrix} \end{aligned} \qquad s \in [-1, 0]$$

and

$$\begin{aligned} \kappa_1^*(r) &= \tfrac{n_1(r) + n_2(r)}{2} = \begin{pmatrix} \operatorname{Re}\left(e^{-i\omega_n \tilde{\tau} \mathrm{r}}\right) \\ \operatorname{Re}\left(\vartheta e^{-i\omega_n \tilde{\tau} r}\right) \end{pmatrix} \\ \kappa_2^*(r) &= \tfrac{n_1(r) - n_2(r)}{2i} = \begin{pmatrix} \operatorname{Im}\left(e^{-i\omega_n \tilde{\tau} r}\right) \\ \operatorname{Im}\left(\vartheta e^{-i\omega_n \tilde{\tau} r}\right) \end{pmatrix} \end{aligned} \qquad r \in [0, 1]$$

Subsequently, we can calculate

$$D_1^* := (\kappa_1^*, \Theta_1), D_2^* := (\kappa_1^*, \Theta_2), D_3^* := (\kappa_2^*, \Theta_1), D_4^* := (\kappa_2^*, \Theta_2).$$

Define

$$(\kappa^*, \Theta) = \left(\kappa_j^*, \Theta_k\right) = \begin{pmatrix} D_1^* & D_2^* \\ D_3^2 & D_4^* \end{pmatrix}$$

and create a new basis $\kappa$ for $P^*$ by

$$\kappa = (\kappa_1, \kappa_2)^T = (\kappa^*, \Theta)^{-1} \kappa^*.$$

Then $(\kappa, \Theta) = I_2$. In addition, define $p_n := \left(\beta_n^1, \beta_n^2\right)$, where

$$\beta_n^1 = \begin{pmatrix} \cos \frac{n}{l} x \\ 0 \end{pmatrix}, \quad \beta_n^2 = \begin{pmatrix} 0 \\ \cos \frac{n}{l} x \end{pmatrix}.$$

Additionally, we define

$$c.p_n = c_1 \beta_n^1 + c_2 \beta_n^2, \quad \text{for} \quad c = (c_1, c_2)^T \in C_1$$

and

$$< H, S >:= \frac{1}{l\pi} \int_0^{l\pi} H_1 \overline{S_1} dx + \frac{1}{l\pi} \int_0^{l\pi} H_2 \overline{S_2} dx \quad \text{for} \quad \text{for} H, S \in X$$

and

$$\langle \chi, p_0 \rangle = \left( < \chi, p_0^1 > , < \chi, p_0^2 > \right)^T$$

Rewrite Eq. (1.3) as form

$$\frac{\mathrm{d}H(t)}{\mathrm{d}t} = A_{\tilde{\tau}} H_t + R\left(H_t, \varepsilon\right),$$

where

$$R\left(H_t, \varepsilon\right) = \begin{cases} 0, & \theta \in [-1, 0) \\ P\left(H_t, \varepsilon\right), & \theta = 0 \end{cases}$$

The solution is

$$H_t = \Theta \begin{pmatrix} y_1 \\ y_2 \end{pmatrix} p_n + h\left(y_1, y_2, \varepsilon\right),$$

where

$$\begin{pmatrix} y_1 \\ y_2 \end{pmatrix} = \left(\kappa, < H_t, p_n >\right),$$

and

$$h\left(y_1, y_2, \varepsilon\right) \in P_S C_1, \quad h(0,0,0) = 0, \quad Dh(0,0,0) = 0$$

Then

$$H_t = \Theta \begin{pmatrix} y_1(t) \\ y_2(t) \end{pmatrix} p_n + h\left(y_1, y_2, 0\right)$$

Let $x = y_1 - i y_2$, and notice that $l_1 = \Theta_1 + i\Theta_2$. Then

$$\Theta \begin{pmatrix} y_1 \\ y_2 \end{pmatrix} p_n = (\Theta_1, \Theta_2) \begin{pmatrix} \frac{x+\bar{x}}{2} \\ \frac{i(x-\bar{x})}{2} \end{pmatrix} p_n = \frac{1}{2}\left(l_1 x + \overline{l_1 x}\right) p_n$$

and $h\left(y_1, y_2, 0\right) = h\left(\frac{x+\bar{x}}{2}, \frac{i(x-\bar{x})}{2}, 0\right)$. Eq. (3.12) is

$$\begin{aligned} H_t &= \frac{1}{2}\left(l_1 x + \overline{l_1 x}\right) p_n + h\left(\frac{x+\bar{x}}{2}, \frac{i(x-\bar{x})}{2}, 0\right) \\ &= \frac{1}{2}\left(l_1 x + \overline{l_1 x}\right) p_n + W(x, \bar{x}), \end{aligned}$$

where $W(x, \bar{x}) = h\left(\frac{x+\bar{x}}{2}, \frac{i(x-\bar{x})}{2}, 0\right)$, and $\dot{x} = i\omega_n \tilde{\tau} x + F(x, \bar{x})$, where

$$F(x, \bar{x}) = (\kappa_1(0) - i\kappa_2(0)) < P\left(H_t, 0\right), p_n >$$

Let

$$\begin{aligned} W(x, \bar{x}) &= W_{20} \tfrac{x^2}{2} + W_{11} x\bar{x} + W_{02} \tfrac{\bar{x}^2}{2} + \cdots, \\ F(x, \bar{x}) &= F_{20} \tfrac{x^2}{2} + F_{11} x\bar{x} + F_{02} \tfrac{\bar{x}^2}{2} + \cdots, \end{aligned}$$

then

$$\begin{aligned} H_t(0) =& \frac{1}{2}(x + \bar{x}) \cos\left(\frac{nx}{l}\right) + W_{20}^{(1)}(0)\frac{x^2}{2} + W_{11}^{(1)}(0) x\bar{x} + W_{02}^{(1)}(0)\frac{\bar{x}^2}{2} + \cdots, \\ S_t(0) =& \frac{1}{2}(\zeta x + \bar{\zeta}\bar{x}) \cos\left(\frac{nx}{l}\right) + W_{20}^{(2)}(0)\frac{x^2}{2} + W_{11}^{(2)}(0) x\bar{x} + W_{02}^{(2)}(0)\frac{\bar{x}^2}{2} + \cdots, \\ H_t(-1) =& \frac{1}{2}\left(x e^{-i\omega_n \tilde{\tau}} + \bar{x} e^{i\omega_n \tilde{\tau}}\right) \cos\left(\frac{nx}{l}\right) + W_{20}^{(1)}(-1)\frac{x^2}{2} + W_{11}^{(1)}(-1) x\bar{x} + W_{02}^{(1)}(-1)\frac{\bar{x}^2}{2} + \cdots \end{aligned}$$

and

$$\begin{aligned}\bar{P}_1(H_t,0) &= \frac{1}{\tilde{\tau}}P_1 = \alpha_{20}H_t^2(0)+\alpha_{11}H_t(0)S_t(0)+\alpha_{02}S_t^2(0)+\alpha_{30}H_t^3(0)\\ &\quad +\alpha_{21}H_t^2(0)S_t(0)+\alpha_{12}H_t(0)S_t^2(0)+\alpha_{03}S_t^3(0)+\cdots,\\ \bar{P}_2(H_t,0) &= \frac{1}{\tilde{\tau}}P_2 = \beta H_t(0)S_t(0)+\delta H_t(-1)S_t(0)+\cdots\end{aligned}$$

Where

$$\alpha_{20}=\frac{ab^2}{(b+H^*)^3(1+fS^*)}-d \qquad \alpha_{11}=\frac{-af\left((H^*)^2+2bH^*\right)}{(b+H^*)^2(1+fS^*)^2}-g_1 \qquad \alpha_{02}=\frac{af^2(H^*)^2}{(b+H^*)(1+fS^*)^3}$$

$$\alpha_{30}=\frac{-ab^2}{(b+H^*)^4(1+fS^*)} \qquad \alpha_{21}=\frac{-ab^2f}{(b+H^*)^3(1+fS^*)^2} \qquad \alpha_{12}=\frac{af^2\left((H^*)^2+2bH^*\right)}{(b+H^*)^2(1+fS^*)^3}$$

$$\alpha_{03}=\frac{-af^3(H^*)^2}{(b+H^*)(1+fS^*)^4} \qquad \beta=g_2 \qquad \delta=-g_3$$

Therefore

$$\bar{P}_1(H_t,0)=\cos^2\left(\frac{nx}{l}\right)\left(\frac{x^2}{2}\phi_{20}+x\bar{x}\phi_{11}+\frac{\bar{x}^2}{2}\phi_{02}\right)+\frac{x^2\bar{x}}{2}\left(\phi_1\cos\frac{nx}{l}+\phi_2\cos^3\frac{nx}{l}\right)+\cdots,$$

$$\bar{P}_2(H_t,0)=\cos^2\left(\frac{nx}{l}\right)\left(\frac{x^2}{2}\mu_{20}+x\bar{x}\mu_{11}+\frac{\bar{x}^2}{2}\mu_{02}\right)+\frac{x^2\bar{x}}{2}\mu_1\cos\frac{nx}{l}+\cdots,$$

Then

$$\begin{aligned}<P(H_t,0),p_n> &= \tilde{\tau}\left(\bar{P}_1(H_t,0)\,p_n^1+\bar{P}_2(H_t,0)\,p_n^2\right)\\ &= \frac{x^2}{2}\tilde{\tau}\begin{pmatrix}\phi_{20}\\ \mu_{20}\end{pmatrix}\Lambda+x\bar{x}\tilde{\tau}\begin{pmatrix}\phi_{11}\\ \mu_{11}\end{pmatrix}\Lambda+\frac{\bar{x}^2}{2}\tilde{\tau}(\mu_{02})\Lambda+\frac{x^2\bar{x}}{2}\tilde{\tau}\begin{pmatrix}\sigma_1\\ \sigma_2\end{pmatrix}+\cdots.\end{aligned}$$

with

$$\Lambda=\frac{1}{l\pi}\int_0^{l\pi}\cos^3\left(\frac{nx}{l}\right)dx,$$

$$\sigma_1=\frac{\phi_1}{l\pi}\int_0^{l\pi}\cos^2\left(\frac{nx}{l}\right)dx+\frac{\phi_2}{l\pi}\int_0^{l\pi}\cos^4\left(\frac{nx}{l}\right)dx,$$

$$\sigma_2=\frac{\mu_1}{l\pi}\int_0^{l\pi}\cos^2\left(\frac{nx}{l}\right)dx$$

and

$$\phi_{20} = \frac{1}{2}\left(\alpha_{20} + \alpha_{11}\eta + \alpha_{02}\eta^2\right) \qquad \mu_{20} = \frac{1}{2}\left(\beta\eta + \delta\eta e^{-i\omega\tau}\right)$$

$$\phi_{11} = \frac{1}{4}\left(2\alpha_{20} + \alpha_{11}\left(\eta + \bar{\eta}\right) + 2\alpha_{02}\eta\bar{\eta}\right) \qquad \mu_{11} = \frac{1}{4}\left(\beta(\bar{\eta} + \eta) + \delta\left(\eta e^{i\omega\tau} + \bar{\eta}e^{-i\omega\tau}\right)\right)$$

$$\phi_{02} = \frac{1}{2}\left(\alpha_{20} + \alpha_{11}\bar{\eta} + \alpha_{02}\bar{\eta}^2\right) \qquad \mu_{02} = \frac{1}{2}\left(\beta\bar{\eta} + \delta\bar{\eta}e^{i\omega\tau}\right)$$

$$\begin{aligned}
\phi_1 &= \alpha_{20}\left(W_{11}^1(0) + \frac{W_{20}^1(0)}{2}\right) + \alpha_{02}\left(\eta W_{11}^2(0) + \bar{\eta}\frac{W_{20}^2(0)}{2}\right) \\
&\quad + \alpha_{11}\left(\frac{W_{11}^2(0)}{2} + \frac{W_{20}^2(0)}{4} + \frac{W_{20}^1(0)}{4}\bar{\eta} + \frac{W_{11}^1(0)}{2}\eta\right) \\
\phi_2 &= \frac{3}{8}\alpha_{30} + \frac{\alpha_{21}}{8}(2\eta + \bar{\eta}) + \frac{\alpha_{12}}{8}\left(\eta^2 + 2\eta\bar{\eta}\right) + \frac{3}{8}\alpha_{03}\eta^2\bar{\eta} \\
\mu_1 &= \frac{1}{4}\beta\left(2W_{11}^2(0) + W_{20}^2(0) + W_{20}^1(0)\bar{\eta} + 2W_{11}^1(0)\eta\right) \\
&\quad + \frac{1}{4}\delta\left(2W_{11}^2(0)e^{-i\omega\tau} + W_{20}^2(0)e^{i\omega\tau} + 2\eta W_{11}^1(-1) + \bar{\eta}W_{20}^1(-1)\right)
\end{aligned}$$

and

$$\begin{aligned}
(\kappa_1(0) - i\kappa_2(0)) < P\left(H_t, 0\right), p_n > &= \frac{x^2}{2}\left(\Lambda_1\phi_{20} + \Lambda_2\mu_{20}\right)\Lambda\tilde{\tau} + x\bar{x}\left(\Lambda_1\phi_{11} + \Lambda_2\mu_{11}\right)\Lambda\tilde{\tau} \\
&\quad + \frac{\bar{x}^2}{2}\left(\Lambda_1\phi_{02} + \Lambda_2\bar{\zeta}_{20}\right)\Lambda\tilde{\tau} + \frac{x^2\bar{x}}{2}\tilde{\tau}\left[\Lambda_1\sigma_1 + \Lambda_2\sigma_2\right] + \cdots,
\end{aligned}$$

Then we have $F_{20} = F_{11} = F_{02} = 0$, for $n = 1, 2, 3, \cdots$.
If $n = 0$, we have:

$$F_{20} = \Lambda_1\tilde{\tau}\phi_{20} + \Lambda_2\tilde{\tau}\mu_{20}, \quad F_{11} = \Lambda_1\tilde{\tau}\phi_{11} + \Lambda_2\tilde{\tau}\mu_{11}, \quad F_{02} = \Lambda_1\tilde{\tau}\phi_{02} + \Lambda_2\tilde{\tau}\bar{\zeta}_{20}.$$

And for $n \in \mathbb{N}_0$

$$F_{21} = \tilde{\tau}\left(\Lambda_1\sigma_1 + \Lambda_2\sigma_2\right)$$

From [19], we have

$$\begin{aligned}
\dot{W}(x, \bar{x}) &= W_{20}x\dot{x} + W_{11}\dot{x}\bar{x} + W_{11}x\dot{\bar{x}} + W_{02}\dot{\bar{x}} + \cdots, \\
A_{\tilde{\tau}}W(x, \bar{x}) &= A_{\tilde{\tau}}W_{20}\tfrac{x^2}{2} + A_{\tilde{\tau}}W_{11}x\bar{x} + A_{\tilde{\tau}}W_{02}\tfrac{\bar{x}^2}{2} + \cdots,
\end{aligned}$$

and

$$\dot{W}(x, \bar{x}) = A_{\tilde{\tau}}W + H(x, \bar{x})$$

where

$$\begin{aligned}
H(x, \bar{x}) &= H_{20}\frac{x^2}{2} + W_{11}x\bar{x} + H_{02}\frac{\bar{x}^2}{2} + \cdots \\
&= X_0P\left(H_t, 0\right) - \Phi\left(\kappa, < X_0P\left(H_t, 0\right), p_n > \cdot p_n\right)
\end{aligned}$$

Hence, we have

$$(2i\omega_n\tilde{\tau} - A_{\tilde{\tau}})\, W_{20} = H_{20}, \quad -A_{\tilde{\tau}} W_{11} = H_{11},$$

$$(-2i\omega_n\tilde{\tau} - A_{\tilde{\tau}})\, W_{02} = H_{02},$$

that is

$$W_{20} = (2i\omega_n\tilde{\tau} - A_{\tilde{\tau}})^{-1} H_{20}, \quad W_{11} = -A_{\tilde{\tau}}^{-1} H_{11},$$
$$W_{02} = (-2i\omega_n\tilde{\tau} - A_{\tilde{\tau}})^{-1} H_{02}.$$

Then

$$\begin{aligned} H(x,\bar{x}) =& -\Phi(0)\kappa(0) < P\left(H_t, 0\right), p_n > \cdot p_n \\ =& -\left(\frac{l_1(\theta)+l_2(\theta)}{2}, \frac{l_1(\theta)-l_2(\theta)}{2i}\right)\begin{pmatrix} \Phi_1(0) \\ \Phi_2(0) \end{pmatrix} < P\left(H_t, 0\right), p_n > \cdot p_n \\ =& -\frac{1}{2}\left[l_1(\theta)\left(\Phi_1(0) - i\Phi_2(0)\right) + l_2(\theta)\left(\Phi_1(0) \ \ + i\Phi_2(0)\right)\right] < P\left(H_t, 0\right), p_n > \cdot p_n \\ =& -\frac{1}{2}\left[\left(l_1(\theta)F_{20} + l_2(\theta)\bar{F}_{02}\right)\frac{x^2}{2} + \left(l_1(\theta)F_{11} \ \ + l_2(\theta)\bar{F}_{11}\right)x\bar{x} + \left(l_1(\theta)F_{02} + l_2(\theta)\bar{F}_{20}\right)\frac{\bar{x}^2}{2}\right] + \cdots \end{aligned}$$

Therefore,

$$H_{20}(\theta) = \begin{cases} 0 & n \in \mathbb{N}, \\ -\frac{1}{2}\left(l_1(\theta)F_{20} + l_2(\theta)\bar{F}_{02}\right)\cdot p_0 & n = 0, \end{cases}$$
$$H_{11}(\theta) = \begin{cases} 0 & n \in \mathbb{N}, \\ -\frac{1}{2}\left(l_1(\theta)F_{11} + l_2(\theta)\bar{F}_{11}\right)\cdot p_0 & n = 0, \end{cases}$$
$$H_{02}(\theta) = \begin{cases} 0 & n \in \mathbb{N}, \\ -\frac{1}{2}\left(l_1(\theta)F_{02} + l_2(\theta)\bar{F}_{20}\right)\cdot p_0 & n = 0, \end{cases}$$

and

$$H(x,\bar{x})(0) = P\left(H_t, 0\right) - \Phi\left(\kappa, < P\left(H_t, 0\right), p_n >\right)\cdot p_n,$$

where

$$H_{20}(0) = \begin{cases} \tilde{\tau}\begin{pmatrix} \phi_{20} \\ \mu_{20} \end{pmatrix}\cos^2\left(\frac{nx}{l}\right), & n \in \mathbb{N}, \\ \tilde{\tau}\begin{pmatrix} \phi_{20} \\ \mu_{20} \end{pmatrix} - \frac{1}{2}\left(l_1(0)F_{20} + l_2(0)\bar{F}_{02}\right)\cdot p_0, & n = 0 \end{cases}$$
$$H_{11}(0) = \begin{cases} \tilde{\tau}\begin{pmatrix} \phi_{11} \\ \mu_{11} \end{pmatrix}\cos^2\left(\frac{nx}{l}\right), & n \in \mathbb{N}, \\ \tilde{\tau}\begin{pmatrix} \phi_{11} \\ \mu_{11} \end{pmatrix} - \frac{1}{2}\left(l_1(0)F_{11} + l_2(0)\bar{F}_{11}\right)\cdot p_0, & n = 0. \end{cases}$$

By the definition of $A_{\tilde{\tau}}$, we have

$$\dot{W}_{20} = A_{\tilde{\tau}} W_{20} = 2i\omega_n\tilde{\tau} W_{20} + \frac{1}{2}\left(l_1(\theta)F_{20} + l_2(\theta)\bar{F}_{02}\right)\cdot p_n, \quad -1 \le \theta < 0.$$

That is

$$W_{20}(\theta) = \frac{i}{2i\omega_n\tilde{\tau}}\left(F_{20}l_1(\theta) + \frac{\bar{F}_{02}}{3}l_2(\theta)\right)\cdot p_n + E_1 e^{2i\omega_n\tilde{\tau}\theta},$$

where

$$E_1 = \begin{cases} W_{20}(0) & n = 1, 2, 3, \ldots, \\ W_{20}(0) - \frac{i}{2i\omega_n\tilde{\tau}}\left(F_{20}l_1(\theta) \ \ + \frac{\bar{F}_{02}}{3}l_2(\theta)\right)\cdot p_0 & n = 0. \end{cases}$$

By the definition of $A_{\tilde{\tau}}$, we have for $-1 \le \theta < 0$

$$-\left(F_{20}l_1(0)+\frac{\bar{F}_{02}}{3}l_2(0)\right)\cdot p_0+2i\omega_n\tilde{\tau}E_1-L_{\tilde{\tau}}\left(\frac{i}{2\omega_n\tilde{\tau}}\left(F_{20}l_1(0)+\frac{\bar{F}_{02}}{3}l_2(0)\right)\cdot p_n+E_1e^{2i\omega_n\tilde{\tau}\theta}\right)$$

$$-A_{\tilde{\tau}}E_1-A_{\tilde{\tau}}\left(\frac{i}{2\omega_n\tilde{\tau}}\left(F_{20}l_1(0)+\frac{\bar{F}_{02}}{3}l_2(0)\right)\cdot p_0\right)=\tilde{\tau}\begin{pmatrix}\phi_{20}\\ \mu_{20}\end{pmatrix}-\frac{1}{2}\left(l_1(0)F_{20}+l_2(0)\bar{F}_{02}\right)\cdot p_0.$$

As

$$A_{\tilde{\tau}}l_1(0)+L_{\tilde{\tau}}\left(l_1\cdot p_0\right)=i\omega_0 l_1(0)\cdot p_0$$

and

$$A_{\tilde{\tau}}l_2(0)+L_{\tilde{\tau}}\left(l_2\cdot p_0\right)=-i\omega_0 l_2(0)\cdot p_0$$

we have

$$2i\omega_nE_1-A_{\tilde{\tau}}E_1-L_{\tilde{\tau}}E_1e^{2i\omega_n}=\tilde{\tau}\begin{pmatrix}\phi_{20}\\ \mu_{20}\end{pmatrix}\cos^2\left(\frac{nx}{l}\right),\quad n\in\mathbb{N}_0$$

That is

$$E_1=\tilde{\tau}E\begin{pmatrix}\phi_{20}\\ \mu_{20}\end{pmatrix}\cos^2\left(\frac{nx}{l}\right)$$

where

$$E=\begin{pmatrix}2i\omega_n\tilde{\tau}+d_1\frac{n^2}{l^2}-m_{11} & -m_{12}\\ -g_2v^*+g_3v^*e^{-2i\omega_n\tilde{\tau}} & 2i\omega_n\tilde{\tau}+d_2\frac{n^2}{l^2}\end{pmatrix}^{-1}$$

Similarly, from (3.26), we have

$$-\dot{W}_{11}=\frac{i}{2\omega_n\tilde{\tau}}\left(l_1(\theta)F_{11}+l_2(\theta)\bar{F}_{11}\right)\cdot p_n,\quad -1\leq\theta<0.$$

That is

$$W_{11}(\theta)=\frac{i}{2i\omega_n\tilde{\tau}}\left(l_1(\theta)\bar{F}_{11}-l_1(\theta)F_{11}\right)+E_2.$$

Similarly, we have

$$E_2=\tilde{\tau}E^*\begin{pmatrix}\phi_{11}\\ \mu_{11}\end{pmatrix}\cos^2\left(\frac{nx}{l}\right),$$

where

$$E^*=\begin{pmatrix}d_1\frac{n^2}{l^2}-m_{11} & -m_{12}\\ -g_2v^* & d_2\frac{n^2}{l^2}\end{pmatrix}^{-1}.$$

Thus, we have:

$$c_1(0)=\frac{i}{2\omega_n\tilde{\tau}}\left(F_{20}F_{11}-2\left|F_{11}\right|^2-\frac{\left|F_{02}\right|^2}{3}\right)+\frac{1}{2}F_{21},$$

$$\mu_2=-\frac{\mathrm{Re}\left(c_1(0)\right)}{\mathrm{Re}\left(\lambda'\left(\tau_n^j\right)\right)},\quad \beta_2=2\,\mathrm{Re}\left(c_1(0)\right)$$

$$T_2=-\frac{1}{\omega_n\tilde{\tau}}\left[\mathrm{Im}\left(c_1(0)\right)+\varepsilon_2\,\mathrm{Im}\left(\lambda'\left(\tau_n^j\right)\right)\right].$$

According to Theorem 3.1 mentioned in [21], the nature of the Hopf bifurcation at any critical value $\tau_{j,n}^{+}$ or $\tau_{j,n}^{-}$ is characterized by three coefficients. The coefficient $\mu_2$ determines the direction of the bifurcation: if $\mu_2 > 0$, the Hopf bifurcation is supercritical, meaning that the bifurcating periodic solutions exist for $\mu > 0$; if $\mu_2 < 0$, it is subcritical and the solutions exist for $\mu < 0$. The coefficient $\beta_2$ indicates the stability of these periodic solutions on the center manifold: if $\beta_2 < 0$, the bifurcating periodic solutions are orbitally asymptotically stable, whereas they are unstable if $\beta_2 > 0$. Finally, the coefficient $T_2$ reflects how the period of the solutions changes: if $T_2 > 0$, the period increases, while if $T_2 < 0$, it decreases.

## 5. Simulations and Discussion

In this section, we aim to validate the theoretical results by visualizing the model's dynamics through numerical simulations. To this end, we analyze the system's stability and evolution using two complementary types of representations: bifurcation diagrams, which identify stability transitions as a function of the delay $\tau$, and spatiotemporal plots, which depict the evolution of populations in space and time. All simulations are carried out in MATLAB to numerically solve the model equations and explore its dynamic behavior. The parameters used in the numerical simulations are listed in Table 2. They represent key biological characteristics that influence population dynamics and determine the system's stability.

Table 2: Values of the parameters used in the model simulations.

| $a$ | $b$ | $c$ | $d$ | $f$ | $g_1$ | $g_2$ | $g_3$ | $m$ | $E_1$ | $E_2$ |
|---|---|---|---|---|---|---|---|---|---|---|
| 6.8 | 0.6 | 0.05 | 0.007 | 0.0003 | 0.0152 | 0.0062 | 0.00422 | 0.301 | 0.03 | 0.09 |

The analysis of the system's dynamics begins with the determination of the strictly positive equilibrium $(H^*, S^*)$ by solving the steady-state equations of the model. Substituting the parameter values from Table 2 into Equation (3.2), we obtain $H^* = 197.47475$. To ensure that this equilibrium is well-defined, we substitute this value into the existence condition given by Equation (3.1), yielding $(c + E_1 + dH^*)(b + H^*) - aH^* = -1053.18$. Since this value is negative, the existence condition of the equilibrium is satisfied. Furthermore, this condition guarantees that $A_0 < 0$, and since the coefficients $A_1$ and $A_2$ are positive, we are assured that the quadratic equation associated with $S^*$ has a unique positive solution. We then solve this equation in the form $A_2S^2 + A_1S + A_0 = 0$, with $A_2 = 0.00090$, $A_1 = 3.09763$, and $A_0 = -1053.17898$. The function $f(S) = A_2S^2 + A_1S + A_0$ is graphically represented in Figure 1, where the intersection with the horizontal axis corresponds to the unique solution $S^* = 311.67084$.

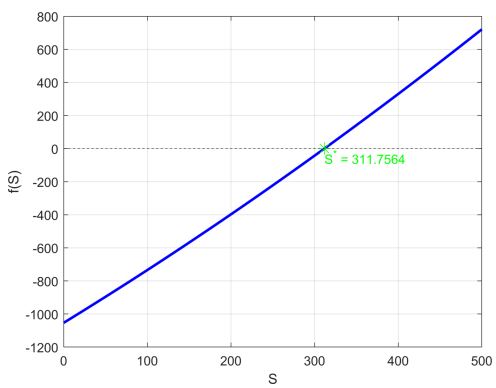


Figure 1: Graphical representation of the quadratic equation associated with $S^*$.

Thus, we obtain the strictly positive equilibrium point of the system, given by $(H^*, S^*) = (197.47475, 311.67084)$, which numerically confirms the coexistence of both species in the studied model.

To numerically analyze the impact of the delay on the system's stability, we constructed two bifurcation diagrams illustrating the evolution of prey and predator populations as functions of $\tau$. These

diagrams make it possible to identify the critical values of the delay beyond which the system undergoes a behavioral transition, particularly from a stable equilibrium to the onset of periodic oscillations. As shown in Figures 2, for $\tau < 1.308$, the system converges to a stable steady state. However, when $\tau$ exceeds this critical threshold, a Hopf bifurcation occurs, giving rise to self-sustained oscillations in the populations.

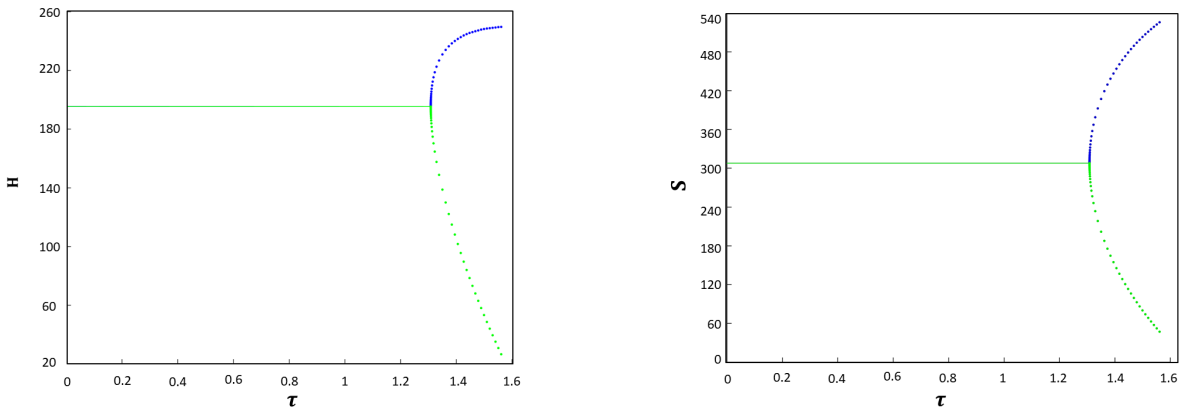


(a) Bifurcation diagram of prey $H$.

(b) Bifurcation diagram of predators $S$.

Figure 2: Transition between stability and oscillations as a function of $\tau$.

From a biological perspective, the stability observed for $\tau < 1.308$ indicates that the prey's anti-predation mechanisms are sufficiently rapid to effectively regulate predator–prey dynamics, thereby maintaining a stable equilibrium. However, when the delay $\tau$ becomes too large, the prey's response to predation pressure is too slow to adequately counter the impact of predators, resulting in cyclic population oscillations. This phenomenon is comparable to natural cycles observed in certain animal populations, where the availability of anti-predation defenses is delayed due to physiological or behavioral constraints.

To better understand the evolution of populations in space and time, we plotted the system's solutions as functions of the spatial variable $x$ and time $t$. These representations illustrate the stability or instability of the system as a function of the delay $\tau$. When $\tau = 0$, the system evolves in a stable manner: the prey and predator densities gradually converge to their equilibrium values without significant oscillations. This indicates that, in the absence of a delay in the anti-predation effect, population dynamics remain well regulated and free of periodic fluctuations. For all simulations presented below, the initial conditions were defined as small spatial perturbations around the equilibrium values, namely $H(x,0) = H^*(1 + \varepsilon\cos(x)\sin(x))$ and $S(x,0) = S^*(1 + \varepsilon\cos(x)\sin(x))$, where $\varepsilon$ denotes a small amplitude.

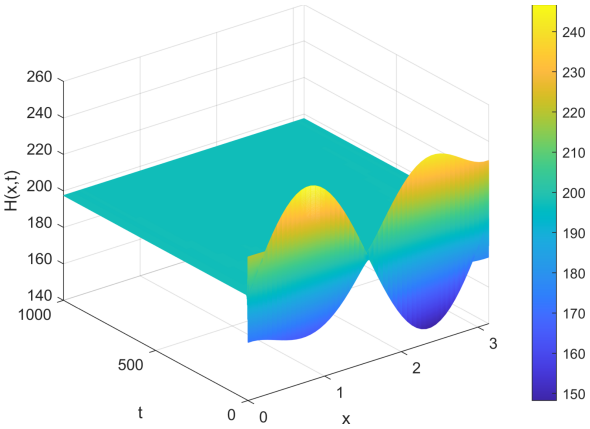


(a) Spatiotemporal evolution of prey $H(x,t)$ for $\tau = 0$.

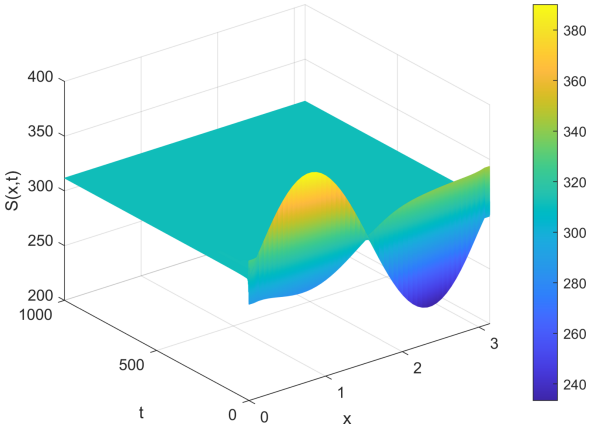


(b) Spatiotemporal evolution of predators $S(x,t)$ for $\tau = 0$.

Figure 3: System dynamics for $\tau = 0$: convergence to equilibrium without oscillations.

When $\tau = 1.4$, the system's dynamics change dramatically. Periodic oscillations emerge in the population densities, indicating a loss of equilibrium stability. These fluctuations demonstrate that delayed anti-predation effects significantly influence the system's behavior by introducing alternating phases of population growth and decline. This behavior is characteristic of a Hopf bifurcation, in which the system transitions from a stable steady state to an oscillatory regime as a consequence of the delay.

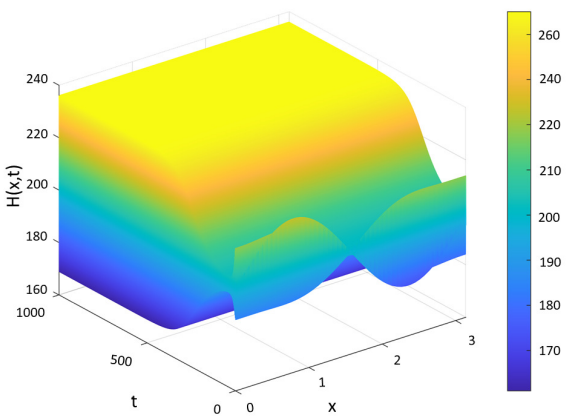


(a) Evolution of $H(x,t)$ for $\tau = 1.4$.

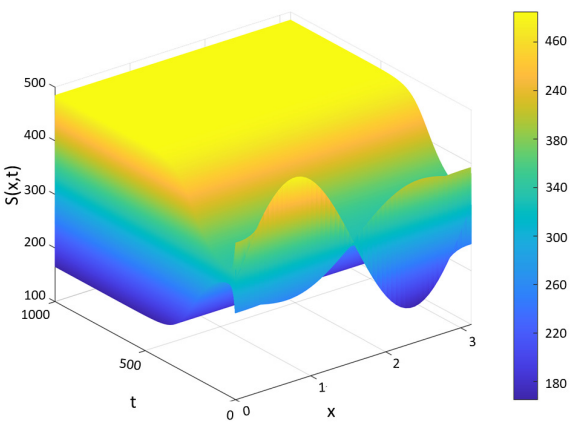


(b) Evolution of $S(x,t)$ for $\tau = 1.4$.

Figure 4: System dynamics for $\tau = 1.4$: emergence of periodic oscillations.

Beyond the effect of the delay, we now analyze the impact of spatial diffusion on the system's dynamics. We first consider a scenario in which the mobilities of prey and predators are relatively similar, with $d_1 = 0.2$ and $d_2 = 0.18$.In this case, the spatial distribution remains homogeneous, and no particular structuring is observed. However, when the prey diffusion rate becomes significantly higher than that of the predators ($d_1 = 1.2$ and $d_2 = 0.01$), the system's dynamics change markedly: spatial patterns emerge, indicating a heterogeneous organization of populations. As shown in Figures 5, the low mobility of predators prevents uniform regulation of the prey population, promoting the formation of aggregation and depletion zones.

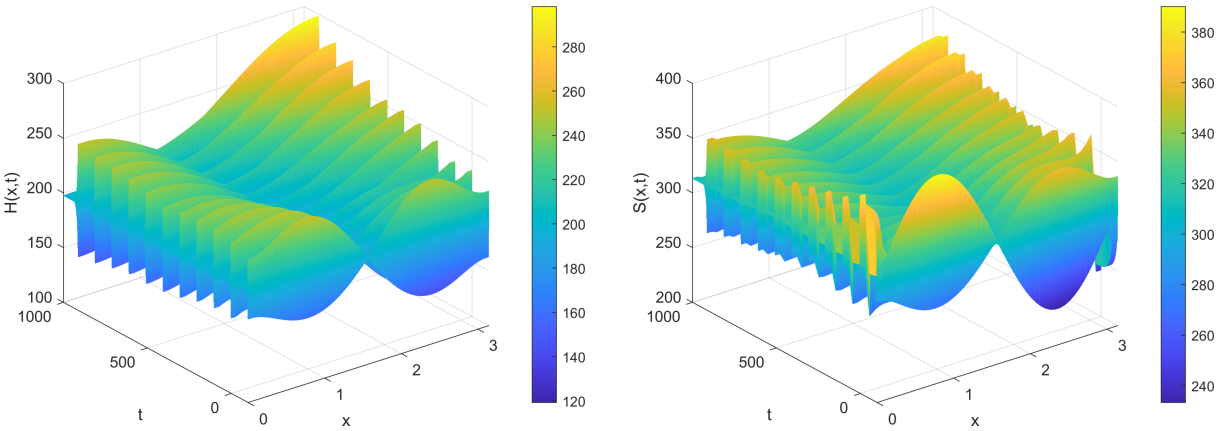


(a) Spatial structures of prey $H(x,t)$. (b) Spatial structures of predators $S(x,t)$.

Figure 5: Formation of spatial structures due to asymmetric diffusion ($d_1 = 1.2$, $d_2 = 0.01$).

The presence of these spatial inhomogeneities resembles phenomena described by the theory of Turing–Hopf bifurcations, where the combination of delayed interactions and unequal diffusion between species promotes the emergence of persistent spatial patterns. These results suggest that the system's dynamics depend not only on the temporal aspects of interactions but also on the capacity of individuals to move and redistribute across space. Such behavior is frequently observed in marine ecosystems, where prey species adopt rapid migration strategies to escape predation.

Our simulations therefore indicate that introducing a delay in the anti-predation response together with an asymmetric diffusion process can profoundly alter system dynamics, affecting not only population stability but also spatial organization. These findings underscore the importance of accounting for both temporal and spatial factors in ecological modeling, as they can have significant implications for the management and conservation of natural ecosystems.

## 6. Conclusion

In this study, we analyzed the dynamics of a predator–prey system by integrating multiple ecological mechanisms often considered separately: the Allee effect, predator-induced fear, delayed anti-predation responses, spatial diffusion, and human harvesting. By introducing a time lag $\tau$, representing the period required for prey to develop defenses, we demonstrated that the system undergoes a Hopf bifurcation beyond a critical threshold, leading to the emergence of periodic population oscillations. The equilibrium analysis confirmed the existence of a strictly positive coexistence state, whose stability was examined through spectral analysis. Furthermore, we explored the characteristics of the Hopf bifurcation using center manifold theory and normal form reduction, providing insight into the nature of the emerging periodic solutions.

Numerical simulations supported these theoretical results, illustrating the transition from stable equilibrium to oscillatory dynamics as the delay increased. Additionally, the inclusion of spatial diffusion revealed that differences in prey and predator mobility could generate spatial heterogeneities, emphasizing the role of movement and dispersal in shaping population distributions. By incorporating harvesting terms, we also assessed the impact of human exploitation on population stability and long-term dynamics.

Overall, the novelty of this work lies in the combined consideration of multiple interacting mechanisms, the Allee effect, fear, delayed anti-predation responses, spatial diffusion, and harvesting, which allows for a more realistic and comprehensive understanding of predator–prey dynamics. Our findings highlight that ecological interactions are not only shaped by immediate predator–prey encounters but are also profoundly influenced by delayed behavioral responses, spatial heterogeneity, and human activities, offering new insights into population management and conservation strategies.

## 7. Conflicts of Interest

The authors declare that there is no conflict of interest regarding the publication of this paper.
The authors declare that there is no funding to disclose.

## References


1. S. Chen, J. Shi, Global stability in a diffusive Holling-Tanner predator-prey model, *Applied Mathematics Letters*, **25**(3) (2012), 614–618.
2. D. Huang, D. Sun, J. Tan, Stability analysis on a predator-prey model with Allee effect, *International Conference on Advanced Material Science and Environmental Engineering (AMSEE 2016)*, (2016), 1–5.
3. L.Y. Zanette, A.F. White, M.C. Allen, M. Clinchy, Perceived predation risk reduces the number of offspring songbirds produce per year, *Science*, **334** (2011), 1398–1401.
4. X. Wang, L. Zanette, X. Zou, Modelling the fear effect in predator–prey interactions, *Journal of Mathematical Biology*, **73** (2016), 1179–1204.
5. S. Pal, S. Majhi, S. Mandal, et al., Role of fear in a predator-prey model with Beddington–DeAngelis functional response, *Zeitschrift f"ur Naturforschung A*, **74** (2019), 581–595.
6. X.N. Liu, L.S. Chen, Complex dynamics of Holling type II Lotka–Volterra predator-prey system with impulsive perturbations on the predator, *Chaos, Solitons & Fractals*, **16** (2003), 311–320.
7. P. Abrams, H. Matsuda, Effects of adaptive predatory and anti-predator behaviour in a two-prey one-predator system, *Evolutionary Ecology*, **7** (1993), 312–326.
8. A.R. Ives, A.P. Dobson, Antipredator behaviour and the population dynamics of simple predator-prey systems, *American Naturalist*, **130**(3) (1987), 431–447.
9. R. Ramos-Jiliberto, E. Frodden, A. Aranguiz-Acu na, Pre-encounter versus post-encounter inducible defenses in predator-prey model systems, *Ecological Modelling*, **200**(1–2) (2007), 99–108.
10. B. Tang, Y. Xiao, Bifurcation analysis of a predator-prey model with anti-predator behaviour, *Chaos, Solitons & Fractals*, **70** (2015), 58–68.
11. X. Sun, Y. Li, Y. Xiao, A predator–prey model with prey population guided anti-predator behavior, *International Journal of Bifurcation and Chaos*, **27**(7) (2017), Article ID 1750099.
12. W. Ko, K. Ryu, Qualitative analysis of a predator-prey model with Holling type II functional response incorporating a prey refuge, *Journal of Differential Equations*, **231**(2) (2006), 534–550.
13. R.R. Patra, S. Maitra, S. Kundu, Stability, bifurcation and control of a predator-prey ecosystem with prey herd behaviour against generalist predator with gestation delay, *arXiv preprint arXiv:2103.16263*, (2021).
14. S. Ghimire, X.-S. Wang, Supercritical Hopf bifurcation of cooperative predation, *arXiv preprint arXiv:2108.09565*, (2021).
15. Y. Yao, T. Song, Z. Li, Bifurcations of a predator-prey system with cooperative hunting and Holling III functional response, *arXiv preprint arXiv:2111.13632*, (2021).
16. Y. Lv, The spatially homogeneous Hopf bifurcation induced jointly by memory and general delays in a diffusive system, *arXiv preprint arXiv:2201.01200*, (2022).
17. M. Hafdane, J.A. Collera, I. Agmour, Y. El Foutayeni, Hopf bifurcation for delayed prey-predator system with Allee effect, *Communications in Mathematical Biology and Neuroscience*, **2023** (2023), Article ID 36.
18. B.D. Hassard, N.D. Kazarinoff, Y.H. Wan, *Theory and Applications of Hopf Bifurcation*, Cambridge University Press, Cambridge, 1981.
19. J. Hale, *Theory of Functional Differential Equations*, Springer, New York, 1977.
20. M. Hafdane, I. Agmour, Y. El Foutayeni, Study of Hopf bifurcation of delayed tritrophic system: dinoflagellates, mussels, and crabs, *Mathematical Modeling and Computing*, **10**(1) (2023), 66–79.
21. F. Liu, R. Yang, L. Tang, Hopf bifurcation in a diffusive predator-prey model with competitive interference, *Chaos, Solitons & Fractals*, **120** (2019), 250–258.
22. J. Wu, *Theory and Applications of Partial Functional Differential Equations*, Springer, Berlin, 1996.
23. B. Xie, Impact of the fear and Allee effect on a Holling type II prey–predator model, *Advances in Difference Equations*, **2021** (2021), Article ID 464.
24. C.V. Pao, On nonlinear reaction-diffusion systems, *Journal of Mathematical Analysis and Applications*, **87**(1) (1982), 165–198.
25. E. S'aez, E. Gonz'alez-Olivares, Dynamics of a predator-prey model, *SIAM Journal on Applied Mathematics*, **59**(5) (1999), 1867–1878.
26. J.T. Tanner, The stability and intrinsic growth rates of prey and predator populations, *Ecology*, **56** (1975), 855–867.

27. Q.X. Ye, Z.Y. Li, *Introduction to Reaction-Diffusion Equations*, Science Press, Beijing, 1990.

28. Guide to the Warder Clyde Allee Papers, *University of Chicago Library*, (1894–1980).

29. S.R.J. Janga, S.L. Diamond, A host–parasitoid interaction with Allee effects on the host, *Computers and Mathematics with Applications*, **53** (2007), 89–103.

30. C. Çelik, O. Duman, Allee effect in a discrete-time predator–prey system, *Chaos, Solitons & Fractals*, **40** (2009), 1956–1962.

31. Alikakos ND. An application of the invariance principle to reaction-diffusion equations. J Differ Equ. (1979) 33:201–25.

32. Kawkab Al Amri, Qamar J. A Khan, David Greenhalgh. Combined impact of fear and Allee effect in predator-prey interaction models on their growth[J]. Mathematical Biosciences and Engineering, 2024, 21(10): 7211-7252. doi: 10.3934/mbe.2024319

33. Yichao Shao, Hengguo Yu, Chenglei Jin, Jingzhe Fang, Min Zhao. Dynamics analysis of a predator-prey model with Allee effect and harvesting effort[J]. Electronic Research Archive, 2024, 32(10): 5682-5716. doi: 10.3934/era.2024263

34. Lingling Li, Xuechen Li. The spatiotemporal dynamics of a diffusive predator-prey model with double Allee effect[J]. AIMS Mathematics, 2024, 9(10): 26902-26915. doi: 10.3934/math.20241309

35. Din Q, Naseem RA, Shabbir MS. Predator–Prey Interaction with Fear Effects: Stability, Bifurcation and Two-Parameter Analysis Incorporating Complex and Fractal Behavior. Fractal and Fractional. 2024; 8(4):221. https://doi.org/10.3390/fractalfract8040221

36. Guin LN, Pal PJ, Alzahrani J, Ali N, Sarkar K, Djilali S, Zeb A, Khan I, Eldin SM. Influence of Allee effect on the spatiotemporal behavior of a diffusive predator-prey model with Crowley-Martin type response function. Sci Rep. 2023 Mar 22;13(1):4710. doi: 10.1038/s41598-023-28419-0. PMID: 36949110; PMCID: PMC10033644.

*M. HAFDANE*[1], *A. IDMBAREK*[1], *N. BABA*[1], *Y. EL FOUTAYENI*[2,3]

(1) *Hassan II University of Casablanca, Morocco*

(2) *Cadi Ayyad University of Marrakech, Morocco*

(3) *Unit for Mathematical and Computer Modeling of Complex Systems, IRD, France*

*E-mail address:* med.hfdn@gmail.com, idmbarekasmaa1@gmail.com, noussaibababa1@gmail.com, foutayeni@gmail.com